IEEE Transactions on Automation Science and Engineering (T-ASE) paper, presented at ICRA 2024, Yokohama, Japan. Cite as T-ASE paper.

Realtime Brain-inspired Adaptive Learning Control for Aircraft with Configuration Uncertainties

Yanhui Zhang*, *Member, IEEE,* Zheyu Tong, Yifan Zhang, Song Chen, Junyuan Yang, Weifang Chen

***Abstract*—This paper investigates the problem of adaptive tracking control for quadcopter in the presence of nonlinear configuration uncertainties. It utilizes a real-time brain-inspired learning control (RBiLC) method to address the challenges posed by nonlinear time-varying uncertain instructions. To address the issue of flight control law reconfiguration caused by unknown changes in the fuselage configuration (e.g., propellers or motors), this paper introduces an online learning-evaluation-optimization reconstruction mechanism based on RBiLC. The proposed adaptive learning controller mitigates the need for extensive human resources and reduces the time required for flight controller design. The Lyapunov-Krasovskii function is introduced as a compensatory measure to address the impact of parameter uncertainty on system stability. Furthermore, this paper proposes a signed sinusoidal function perturbation estimate to guide the direction and magnitude throughout the online learning process. The approach conducts a theoretical stability analysis on a quadcopter vehicle considering uncertainties in UAV dynamics modeling. The results demonstrate that the proposed scheme achieves superior control and faster adaptation, enabling the system to ultimately converge to a compact set within a limited time domain. Finally, software-in-the-loop (SITL) simulations and flight verification results are presented to validate the proposed control strategy.**

***Index Terms*—Real-time adaptive learning control, nonlinear quadcopter control, configuration uncertainties.**

I. Introduction

ADAPTIVE control has been extensively researched for linear system control tasks, utilizing historical response information to improve the control performance of the current controller [1]. However, nonlinear uncertain strict feedback systems are prevalent in practical engineering, as seen in cross-domain flight rocket control systems [2] and unmanned aerial vehicle (UAV) control systems [3], [4]. In such control systems, the real-time uncertain configuration of the plant models can increase control difficulty, leading to system oscillation or divergence. Therefore, this paper aims to study the real-time adaptive learning control problem of nonlinear strict-feedback systems with uncertain configurations to realize a point-by-point response to the desired command. Achieving stable control of multirotor UAVs under different working conditions typically requires redesigning the UAV controllers with different loads and propeller sizes, which is a time-consuming and laborious task. Most recent studies can be mainly categorized into two trends for the control system reconstruction problem. One of them combines model-base method and artificial experience to reconstruct the controller parameters offline, such as model reference adaptive control (MRAC) [5], fault-tolerant control systems (FTCS) [6], retrospective cost adaptive control (RCAC) [7], model predictive control (MPC) [8] and H_∞ control [9]. The other trend in control is to employ a model-free approach to address these problems. The earliest model-free control methods can be traced back to proportional-integral-derivative (PID) control [10]. Since then, several model-free control approaches have been developed, including extremum seeking (ES) [11], Ziegler-Nichols-PID (ZN-PID) [12], PID-ES [13], model-free adaptation control (MFAC) [14], event-triggered adaptive control [15], and iterative learning control (ILC) [16]. Our previous work has also explored the nonlinear parameter strict feedback system control method of ILC for a class of unknown state delays in [17]. In addition, ILC was utilized to learn the controller of a closed-loop UAV system in [18]. On this basis, some model-free intelligent learning control methods have been proposed to be applied to UAVs. To name just a few, in [19], robust transform-based real-time adaptive intelligent control is used to offset the parametric uncertainty of the quadcopter and improve the stability under external disturbances. Reinforcement learning (RL) is implemented in [20], enabling the controller to learn when multiple actuators fail. Later, a domain adversarially invariant meta-learning (DAIML) method is proposed to solve this problem in [21]. Their approach combines adaptive flight and reinforcement learning-based robot control. As mentioned in [22], [23], future spacecraft also need to quickly and accurately deal with the control problems caused by spacecraft configuration changes, such as aerodynamics and loads changes. Typically, experts learn to migrate controller parameters based on experience in threefold, instruction tracking response, performance evaluation, and controller iterative refactoring.

In this paper, a real-time brain-inspired learning control (RBiLC) scheme is proposed, which consists of three steps: iterative instruction response, performance evaluation, and control parameter reconstruction. Moreover, we establish an appropriate Lyapunov-Krasovskii function to ensure that the

This work was supported in part by the China Scholarship Council (grant number 202306320387) and the National Natural Science Foundation of China under Grant U20B2007 and Grant 12002306. (*Corresponding author: Weifang Chen.*)

Y. Zhang, Z. Tong, Y. Zhang, J. Yang and W. Chen are with the School of Aeronautics and Astronautics, Zhejiang University, Hangzhou, China; Y.Zhang and S. Chen also a CSC Ph.D visiting student for the Department of Electronics and Computer Engineering at the National University of Singapore. S. Chen (e-mail: anhuizhang91@gmail.com; chenwfnudt@163.com).

IEEE Transactions on Automation Science and Engineering (T-ASE) paper, presented at ICRA 2024, Yokohama, Japan.

controller structure converges to a compact set through iterative evolution during learning. Compared to existing work, our work's main contributions are:

1) A weak model-dependent brain-inspired adaptive learning reconstruction control algorithm is proposed which is based on self-supervised extremum-seeking. Unlike deep learning schemes, this learning process is interpretable and real-time.
2) A real-time cost evaluation function is developed to guide the controller parameters toward the optimal values. To mitigate the impact of wind disturbance, a digital wind direction measurement and anemometer hardware are connected to the ground station. They evaluate the external wind disturbance and incorporate it into the wind disturbance control compensation.
3) An adaptive extremum seeking method incorporating deep learning momentum acceleration is introduced into the RBiLC framework to achieve interpretability of the learning process. Furthermore, a stability theory proof is achieved based on the established Lyapunov-Krasovskii function.
4) A software-in-the-loop (STIL) simulations and real-world experiments are conducted to evaluate wind field disturbance cancellation in the learning process, considering disturbed wind fields and wind field measurements.
5) Finally, the proposed RBiLC algorithm is employed for online adaptive learning during real-world quadcopter flight, enabling the system to adapt to unknown configuration changes in the propellers or motors.

The rest of this paper is organized as follows. Section II formalizes the adaptive learning tracking control problem for a class of nonlinear systems with uncertain configurations, and this section reviews some necessary assumptions and mathematical tools. Section III presents the detailed design process of the brain-inspired adaptive learning controller and rigorously proves the stability of the control system. In Section IV, the effectiveness of the RBiLC is confirmed by SITL simulation, and real-world experiment in Section V. Section VI summarizes this work and gives an outlook for future research.

Notaion: R and N denote the sets of real numbers and positive integers, respectively. Ri represents the set of i-dimensional real vectors. $P(\cdot)$ is the projection operator, which will be defined later.

II. Preliminaries

In this section, some basic concepts and results of UAV adaptive control systems are introduced, and basic problem descriptions are given. Consider a class of nonlinear dynamic systems with configuration unceratainties as follows:

$$\begin{cases} \boldsymbol{x}^n(t) = \boldsymbol{f}(\boldsymbol{x}(t)) + \boldsymbol{g}(\boldsymbol{x}(t))\boldsymbol{u}(t) + \boldsymbol{w}(t) \\ \boldsymbol{y}(t) = \boldsymbol{h}(\boldsymbol{x}(t)) \end{cases} \tag{1}$$

where $\boldsymbol{u}(t) \in \mathbb{R}^n$, $\boldsymbol{y}(t) \in \mathbb{R}^n, \boldsymbol{x}(t) \in \mathbb{R}^m, \boldsymbol{w}(t) \in \mathbb{R}^m$ respectively represent the system control vector, system output vector, system state vector and unknown external disturbance mapping in the Euclidean space. $\boldsymbol{x}^n(t)$ denotes the n order derivative, $\boldsymbol{f}(\boldsymbol{x}(t)) : \mathbb{R}^n \to \mathbb{R}^n$ and $\boldsymbol{g}(\boldsymbol{x}(t)) : \mathbb{R}^n \to \mathbb{R}^n$ are nonlinear uncertain Lipschitz continuous functions.

In general, the multi-channel coupling control problem of UAV is always decoupled into multiple single-channel control problems as shown in [24]- [25]. The common fixed structure PID controller is defined as follows:

$$\boldsymbol{u}(t)_j = K_p^j \boldsymbol{e}(t) + K_i^j \int_0^t \boldsymbol{e}(\tau)d\tau + K_d^j \dot{\boldsymbol{e}}(t) \tag{2}$$

where K_p^j, K_i^j, K_d^j present proportional, integral and derivative terms of different channels controller gains, and $j \in [\phi, \theta, \psi]$. The performance function of nonlinear system controller with uncertain configurations can defined as

$$J^*(x(t)) = \arg \min_{u \in \mathscr{A}(\Omega)} \int_t^\infty (\mathcal{S}(x(\tau)) + U^*(x(\tau), u(\tau)))\mathrm{d}\tau. \tag{3}$$

The purpose of this paper is to get the system output $y(x)$ tending to the expected output $y^*(x)$ by updating the optimal cost corresponding $J^*(x)$ to the controller structure $U^*(x)$.

The UAV control system has a problem of control channel coupling, which is usually addressed by decoupling it into single-channel processing.

Assuming that the optimal cost of the system for different dynamical model configurations can be formulated as a second-order Taylor expansion of J at the optimal compensation factor $\mathbf{K}^*$ with

$$\lim_{u \to u^*} J(\mathbf{K}^*) = 0. \tag{4}$$

The error of estimation defined as $\tilde{K} = K^* - \hat{K}$, and the optimal performance function can be described as $f(K)^*$.

III. Real-time brain-inspired adaptive learning controller

In this section, a real-time brain-inspired adaptive learning controller is presented for nonlinear system by following the design procedure of the adaptive learning method, where the Lyapunov-Krasovskii functions are employed to compensate for the uncertain configuration of the system. On this basis, the stability of the control system and the convergence of the command tracking error are proved by setting a suitable performance cost function.

A. RBiLC design

In this work, the brain-inspired process is utilized to calculate the controller's globally stabilized structure $\mathbf{K}(t) = [\mathbf{K}_p(t), \mathbf{K}_i(t), \mathbf{K}_d(t)]$ for unknow multirotor as shown in Fig. 1.

B. Theoretical Analysis

Before conducting the stability analysis of the online control of the nonlinear configuration uncertain system, we first need to make some assumptions.

IEEE Transactions on Automation Science and Engineering (T-ASE) paper, presented at ICRA 2024, Yokohama, Japan.

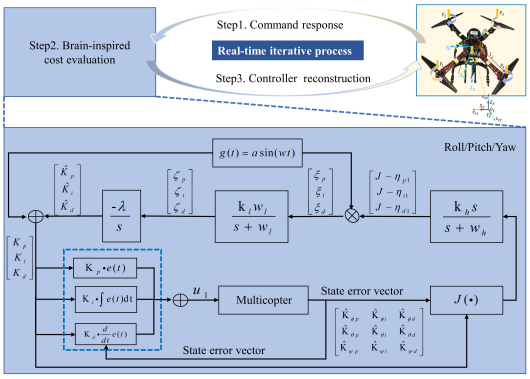

Fig. 1. Scheme of adaptive controller for multicopter. Our study achieves real-time reconfiguration of the controller by estimating the controller's optimal structural parameter matrix $\mathbf{K}^*$. A time-dependent sinusoidal signal with direction $g(t)$ is superimposed in each iteration step based on the controller estimate $\hat{\mathbf{K}}$ from the previous step as the next controller structural parameter $\mathbf{K}$, and u_1 is the output of flight controller.

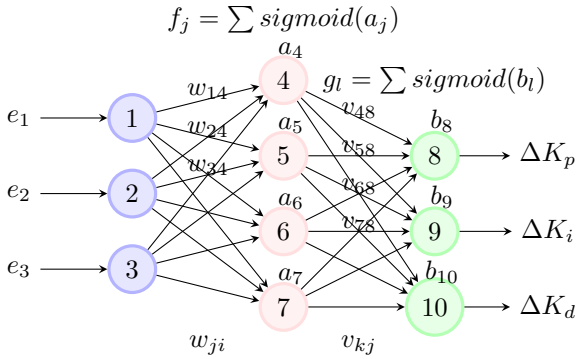

Fig. 2. Schematic diagram of the human brain learning controller parameters iteratively in real time. $e_i, (i = 1, 2, 3)$ denotes the regulation error of three attitude channels, and ΔK present the system control parameters increment.

Assumption 1. *Define the transforms function as $\mathcal{M} = M(x)$, and one can rewrite the nonlinear control system (1) as follows*

$$\begin{cases} \dot{z}_i = z_{i+1}, & i = 0, \ldots, n-1 \\ \dot{z}_n = f(z) + g(z)u(t) + w(t), \\ y = z_1. \end{cases} \tag{5}$$

where $z^* \triangleq (y^*, 0, \ldots, 0)^T \in \mathbb{R}^n$, and $m \in \mathbb{R}^n$, $J_M(\cdot)$ presents the Jacobian matrix of map $M(x) : \mathbb{R}^n \to \mathbb{R}^n$.

$$M(x) = (h(x), \sum_{i=1}^{n} \frac{\partial h}{\partial x_i}(x) f_i(x), \ldots, \sum_{i=1}^{n} (\frac{\partial h}{\partial x_i}(x))^n f_i(x))^T. \tag{6}$$

For any setpoint $y^*(t)$, there always exists increasing function f_1, f_2 from $\mathbb{R}^+ \to \mathbb{R}^+$ with $\limsup_{x\to 0} \frac{f_1(x)}{x} < \infty$ and $\limsup_{x\to 0} \frac{f_2(x)}{x} < \infty$.

IV. Simulation Verification

Software in the loop (SITL) simulation is performed to validate the effectiveness of the proposed brain-inspired learning control scheme in this section. The simulation platform was built on Ubuntu18.04.6 LTS system, with the hardware

Algorithm 1 RBiLC Algorithm for Attitude Control

Input:
Initialization: attitude controller parameters:
$\mathbf{K}_p(0) = [K_{\phi,p}(0), K_{\theta,p}(0), K_{\psi,p}(0)]^\top$;
$\mathbf{K}_i(0) = [K_{\phi,i}(0), K_{\theta,i}(0), K_{\psi,i}(0)]^\top$;
$\mathbf{K}_d(0) = [K_{\phi,d}(0), K_{\theta,d}(0), K_{\psi,d}(0)]^\top$;
$J(k)$: cost function value in time k, $J(0) = 0$;
Hyperparameters:
$\eta_0 = 0.5$: overshoot coefficient;
$\alpha_0 = 0.2$: brain inspire learning rate ;
$\lambda = 0.6$: adaptive gain;
δ_0: sample time;
k_{max}: the maximum cycle of learning;
Output:
$U_{\phi,\theta,\psi}(K(k)) = [E((k-1)), \sum_{i=0}^{m_k} E(i) \cdot \Delta t, \frac{E(k)-E(k-1)}{\Delta t}] \cdot \mathbf{K}(k-1)$.

Adaptive learning process
for channels number $j = 1 : 3$ **do**
  for iter number $k = 1 : k_{(j,max)}$ **do**
    Check attitude level;
    if attitude is level &$J_j(k) > J_j{}^*$ **then**
      $J_j(k) \leftarrow$ cost value as shown in (**??**);
    $\nabla \mathbf{K}_j(k) \leftarrow$ parameters change estimator from (**??**);
    $\mathbf{Y}_j(k) \leftarrow$ do action $(-1)^k [\phi_d, \theta_d, \psi_d]_j^\top$;
    back to level;
    k++;
    Update $U_j(K(k))$;
    else
      Wait back to level();
      Update $U_j(K(k)) = U_j(K(0))$;
  while The learning process is interrupted **do**
    Baseline controller takeover;
    Update $U_j(K(k))$;
Logging $\mathbf{K_j}^*$;
return $U_{\phi,\theta,\psi}(K(k))$.

configuration as 11th Gen Intel Core i7-11800H@2.30GHz*16 and disk as 151.0G. The quadcopter model is simulated with X-type as shown in Fig. **??**. The ground control station (GCS) uses the open source ground station Mission Planer running on Windows 10 and connecte with a quadcopter using MAVProxy by Local Area Network (LAN).

V. Experimentation

In order to verify the effectiveness of the proposed method, we built an X-type quadcopter flight platform based on the F450 frame with the following specific parameters: 2312kv brushless motor, Hobbywing 20A brushless electronic speed controller (ESC), flight controller hardware, UAV body frame, battery, 9450 self-locking propeller and 9455 noise-reducing folding three-blade propellers.

1) UAV design: We designed two aerodynamic characteristics of the propeller (2-blade and 3-blade) to simulate an uncertain variation of the UAV power system model. Without relying on a priori knowledge of the UAV, real-time controller

IEEE Transactions on Automation Science and Engineering (T-ASE) paper, presented at ICRA 2024, Yokohama, Japan.

reconfiguration can be achieved for different models using only real-time aerial learning data.

The 2-blade propeller (APC material) radius is $r_1 = 119.38$mm, pitch is $c_1 = 127$mm and weight is $w_1 = 11.3$g. The 3-blade propeller (carbon fiber material) radius is $r_2 = r_1 = 119.38$mm, pitch is $c_2 = 139.7$mm, weight is $w_2 = 35$g, and the 3-blade propeller tip is optimized for noise reduction. For external random wind disturbance, the wind speed and direction of the flight site need to be measured in real-time. However, the existing equipment in the market can not realize the automatic cooperative measurement of wind direction and speed. Then we designed and built a universal real-time wind direction anemometer based on a normal anemometer. It can automatically follow the maximum wind direction steering to measure the test flight environment.

Fig. 3. The fully automatic realtime aerovane.

All experiments were conducted outdoors as shown in Fig. 4, the aircraft positioning system based on a Global Positioning System (GPS) module, the data transmission link based on a WIFI module, and the remote control link based on the open source OPEN TX system with SBUS protocol.

2) Case A: Learning Under 2-blade Propeller Configuration: The 2-blade propeller adopts a 9450 self-locking plastic paddle. The control effect of manual experience for parameter adjustment is used as the baseline. Then the RBiLC is intervened for learning control. Finally, the control effect is compared, and the quantitative indexes are selected as rising time overshoot and average cumulative error.

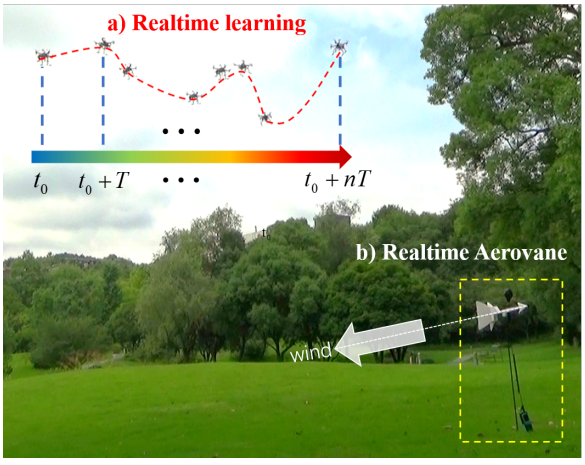

Fig. 4. Outdoor flight test of RBiLC for quadcopter uncertain model platform. In a): t_0 denotes the time of learning start time, and T denotes the periodic time of random step singal, n denotes the max number of iteration learning. In b): In real-time, the wind vane can record the relative air speed in the direction of the maximum wind speed in the outdoor random wind field.

The excitation response process of the UAV under various unknown configuration model conditions was recorded by the on-board camera. It was observed that at different heights with the same horizontal position, high-altitude obstructions are reduced while wind disturbance is more significant, and the low-altitude wind is relatively weak. Therefore, high-altitude aircraft require a particular wind compensation inclination command to maintain a horizontal position. Additionally, when the periodic command returns to zero, it is necessary to superimpose the wind disturbance compensation command based on the horizontal attitude.

$$[\phi, \theta, \psi]_{cmd} = [\phi, \theta, \psi]_{level} + [\phi, \theta, \psi]_{desire}, \tag{7}$$

where $[\phi, \theta, \psi]_{cmd}$ represent the real desire command angles send to attitude controller, $[\phi, \theta, \psi]_{level}$ represent measure-level angles, and $[\phi, \theta, \psi]_{desire}$ represent the relative desire angles.

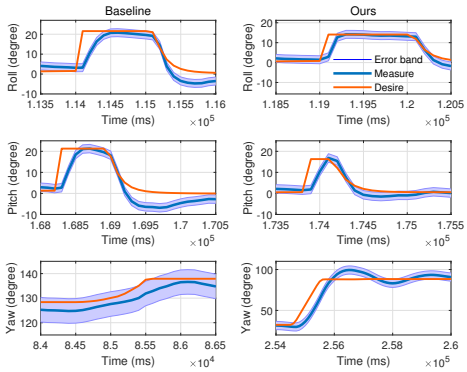

Fig. 5. 2-blade in real-world: attitude tracking response of self-learning. The left output curve are the step responses of $[\phi, \theta, \psi]$ for the model-free controller designed based on ZN rules, and the right are the step response used RBiLC method.

The disadvantage of the ZN method is that the optimal controller reconstruction design needs to be carried out through multiple manual offline trials and errors for unknown control models. In contrast, the RBiLC method can significantly reduce the rise time and the overshoot of the roll and pitch channels' responses. It should be noted, however, that due to wind compensation, the yaw channel may experience partial overshoot when tracking large orders exceeding 50°, but the rise time has been significantly improved.

Comparing the attitude tracking learning effect of the RBiLC controller with that based on the ZN method using the data presented in Figure 5, we can observe that RBiLC reduces the rise time of all three attitude channels by at least 38.46%. Additionally, overshoot is also reduced in this experimentation.

To downscale the 9-dimensional space solution problem to a 3-dimensional one and reduce the complexity of channel coupling, independent learning is carried out in the order of roll, pitch, and yaw. This is achieved by updating the controller parameters through each iteration of the cost function, as shown in Figure 6.

3) Case B: Learning Under 3-blade Propeller Configuration: The learning experiment of the 2-blade propeller can

IEEE Transactions on Automation Science and Engineering (T-ASE) paper, presented at ICRA 2024, Yokohama, Japan.

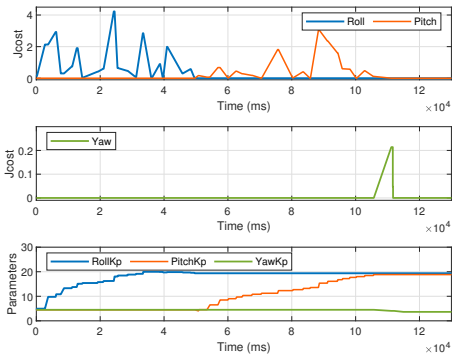

Fig. 6. 2-blade in real-world: the cost value and the controller parameters of roll, pitch, yaw (ϕ, θ, ψ) during the attitude controller self-learning.

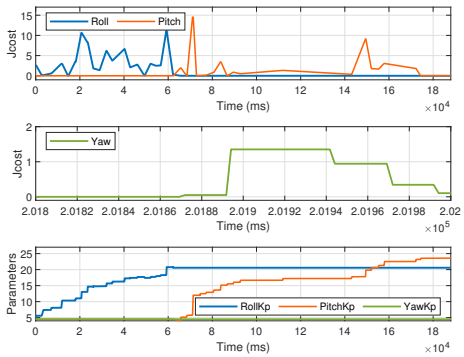

Fig. 8. 3-blade in real-world: the cost value and the controller parameters of roll, pitch, yaw (ϕ, θ, ψ) during the attitude controller self-learning.

fully demonstrate the effectiveness of the learning process. However, to more effectively illustrate that this method is also effective when dealing with UAVs with unknown configurations or uncertain physical models, we designed a 3-blade carbon fiber propeller with an unknown model to conduct control reconstruction experiments on the same body with learning while flying.

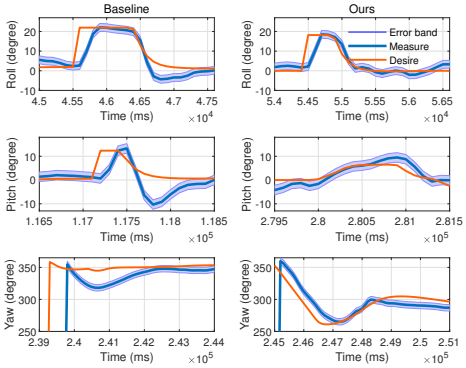

Fig. 7. 3-blade in real-world: attitude tracking response of self-learning. The left output curve are the step responses of $[\phi, \theta, \psi]$ for the model-free controller designed based on ZN rules, and the right are the step response used RBiLC method.

As can be seen from the Fig. 7, the attitude control system roll and yaw channel overshoot after learning have been significantly lower. At the same time, in order to resist gusts, the aircraft equilibrium state needs a roll angle to counteract the wind disturbance. Then there will be a problem of small final equivalent attitude instructions and slow iteration of controller parameters, we solve by expanding the maximum number of iterations and accelerating the historical momentum. In the Fig. 8, after a sufficient number of iterations, the performance cost function of the system may fluctuate or stagnate in gusty conditions but may eventually be J^*.

Based on $CaseA$ in above, we only replace the propeller of the unknown dynamic model and simulate the controller adaptive reconstruction learning process under the unknown configuration. Fig. 8 shows that after about 3∼5 minutes of learning, the overall performance cost tends to be zero. Combined with the automatic heading adjustment compensation mechanism to the wind direction, the standard step response is excessively soft variable step instructions, thereby reducing wind field interference and realizing pilot test flight debugging without manual intervention.

We also conducted flight experiments to compare the attitude and motor output changes before and after the UAV dropped the package with or without the quadcopter controller turning on the self-learning function. The results show that the learning controller can easily cope with the random system perturbations caused by the parcel drop and can quickly and stably restore a smooth flight.

VI. Conclusion

In this paper, a real-time brain-inspired learning control (RBiLC) algorithm is developed to solve the multi-rotor control problem in a class of nonlinear systems with unknown configurations. A cost function, similar to the control effect evaluation of the human brain, is used to guide the adaptive reconstruction of the controller parameters in real-time to obtain the UAV controller fitting for the unknown configuration. The algorithm's logic and effectiveness are verified in the SITL environment and deployed on a quadcopter in a natural wind disturbance environment for actual flight. The results demonstrate that the RBiLC can reduce the rise time by at least 30%, decrease the overshoot response by 20%, and, most importantly, reduce the full process controller reconfiguration time. It can also learn controller parameters for $[\phi, \theta, \psi]$ in 3∼5 minutes. Future work will incorporate tiltable vertical takeoff and landing vehicles (VTOL) into the adaptive learning framework to minimize the design of flight controllers with varying model parameters.

Acknowledgments

This paper acknowledges the valuable contributions of Prof. Chao Xu during the revision of the paper, as well as the contributions of Dr. Hua Yang during the experimental stage. The authors are grateful for their efforts and support.

IEEE Transactions on Automation Science and Engineering (T-ASE) paper, presented at ICRA 2024, Yokohama, Japan.

TABLE I
3 AXIS ATTITUDE (ϕ, θ, ψ) PERFORMANCE COMPARISON

Case	Method	Rise time(Second)	Overshoot(%)	Controller Gains
SITL	Baseline1-ZN-PID	[0.75, 0.42, 0.9]	[0, 2.01, 0]	[4.53, 4.53, 4.41]
	Ours-RBiLC	[0.42, 0.21, 0.35]	[0, 1.53, 3.12]	[22.84, 21.53, 4.04]
	$\sigma_p(\%)$	[56.67↓, 52.32↓ , 61.11↓]	[0,23.88↓, 3.12↑]	[↑, ↑, ↓]
Two-blade RW	Baseline2-ZN-PID	[0.52, 0.26, 0.47]	[5.12, 8.23, 0]	[4.53, 4.53, 4.41]
	Ours-RBiLC	[0.31, 0.16, 0.21]	[2.01, 3.32, 10.26]	[19.8, 19.6, 3.8]
	$\sigma_p(\%)$	[40.38↓, 38.46↓, 55.31↓]	[60↓,62.5↓, 10.26↑]	[↑, ↑, ↓]
Three-blade RW	Baseline3-ZN-PID	[0.36, 0.42, 0.23]	[3.68, 6.15, 39.12]	[4.24, 4.24, 4.50]
	Ours-RBiLC	[0.25, 0.28, 0.11]	[1.71, 3.03, 20.78]	[20.13, 22.82, 4.10]
	$\sigma_p(\%)$	[30.56↓, 33.33↓ , 52.17↓]	[53.53↓,50.73↓, 46.89↓]	[↑, ↑, ↓]

1. RW in *Two-blade RW and Three-blade RW represents Real World expriments, ZN represents the Ziegler-Nichols method.*
2. Relative change σ_p between ZN-PID and RBiLC was defined as $\sigma_p = (V_{ZNPID} - V_{RBiLC})/V_{RBiLC}$, and V denotes as the value of rise time and the overshoot.
3. To simplify the learning process, we set the integral terms k_i and differential terms k_d in the whole process to remain immovable for the time being, taking a value of 0.01.

REFERENCES

[1] H. Anfinsen and O. M. Aamo, "Adaptive control of linear 2x2 hyperbolic systems," *Automatica*, vol. 87, pp. 69–82, 2018.

[2] Z. Wang, W. Bao, and H. Li, "Second-Order Dynamic Sliding-Mode Control for Nonminimum Phase Underactuated Hypersonic Vehicles," *IEEE Transactions on Industrial Electronics*, vol. 64, no. 4, pp. 3105–3112, Apr. 2017.

[3] X. Dong, Y. Hua, Y. Zhou, Z. Ren, and Y. Zhong, "Theory and experiment on formation-containment control of multiple multirotor unmanned aerial vehicle systems," *IEEE Transactions on Automation Science and Engineering*, vol. 16, no. 1, pp. 229–240, 2019.

[4] Y. Zhang, H. Yang, Y. Chen, and W. Chen, "Adaptive extremum seeking controller via nonlinear variable gain for uncertainty model multirotor," in *2022 41st Chinese Control Conference (CCC)*, 2022, pp. 2308–2314.

[5] M. Jin, J. Lee, and N. G. Tsagarakis, "Model-Free Robust Adaptive Control of Humanoid Robots With Flexible Joints," *IEEE Transactions on Industrial Electronics*, vol. 64, no. 2, pp. 1706–1715, Feb. 2017.

[6] Y. Zhang and J. Jiang, "Bibliographical review on reconfigurable fault-tolerant control systems," *Annual Reviews in Control*, vol. 32, no. 2, pp. 229–252, Dec. 2008.

[7] S. A. U. Islam, T. W. Nguyen, I. V. Kolmanovsky, and D. S. Bernstein, "Data-driven retrospective cost adaptive control for flight control applications," *Journal of Guidance, Control, and Dynamics*, vol. 44, no. 10, pp. 1732–1758, 2021.

[8] A. T. Hafez, A. J. Marasco, S. N. Givigi, M. Iskandarani, S. Yousefi, and C. A. Rabbath, "Solving multi-uav dynamic encirclement via model predictive control," *IEEE Transactions on Control Systems Technology*, vol. 23, no. 6, pp. 2251–2265, 2015.

[9] H. Wang, Z. Li, H. Xiong, and X. Nian, "Robust H∞ attitude tracking control of a quadrotor UAV on SO(3) via variation-based linearization and interval matrix approach," *ISA Transactions*, vol. 87, pp. 10–16, 2019.

[10] Y. Zhang, T. Chen, S. Chen, and Z. Wang, "Assess-ranging-fuse: Obstacle detection based on stereo vision threat assessment and ultrasonic ranging," in *2020 Chinese Automation Congress (CAC)*, 2020, pp. 6186–6191.

[11] D. Zhou, A. Al-Durra, I. Matraji, A. Ravey, and F. Gao, "Online Energy Management Strategy of Fuel Cell Hybrid Electric Vehicles: A Fractional-Order Extremum Seeking Method," *IEEE Transactions on Industrial Electronics*, vol. 65, no. 8, pp. 6787–6799, 2018.

[12] J. G. Ziegler and N. B. Nichols, "Optimum Settings for Automatic Controllers," *Journal of Dynamic Systems, Measurement, and Control*, vol. 115, no. 2B, pp. 220–222, 06 1993.

[13] N. Killingsworth and M. Krstic, "PID tuning using extremum seeking: Online, model-free performance optimization," *IEEE Control Systems Magazine*, vol. 26, no. 1, pp. 70–79, 2006.

[14] Q. Wei, L. Zhu, R. Song, P. Zhang, D. Liu, and J. Xiao, "Model-Free Adaptive Optimal Control for Unknown Nonlinear Multiplayer Nonzero-Sum Game," *IEEE Transactions on Neural Networks and Learning Systems*, vol. 33, no. 2, pp. 879–892, Feb. 2022.

[15] Q. Hou and J. Dong, "Cooperative Fault-Tolerant Output Regulation of Linear Heterogeneous Multiagent Systems via an Adaptive Dynamic Event-Triggered Mechanism," *IEEE Transactions on Cybernetics*, pp. 1–12, 2022.

[16] Z. Cao, H.-B. Dürr, C. Ebenbauer, F. Allgöwer, and F. Gao, "Iterative Learning and Extremum Seeking for Repetitive Time-Varying Mappings," *IEEE Transactions on Automatic Control*, vol. 62, no. 7, pp. 3339–3353, Jul. 2017.

[17] Y. Chen, D. Huang, N. Qin, and Y. Zhang, "Adaptive Iterative Learning Control for a Class of Nonlinear Strict-Feedback Systems With Unknown State Delays," *IEEE Transactions on Neural Networks and Learning Systems*, pp. 1–12, 2021.

[18] W. He, T. Meng, X. He, and C. Sun, "Iterative Learning Control for a Flapping Wing Micro Aerial Vehicle Under Distributed Disturbances," *IEEE Transactions on Cybernetics*, vol. 49, no. 4, pp. 1524–1535, Apr. 2019.

[19] P. K. Muthusamy, M. Garratt, H. Pota, and R. Muthusamy, "Real-Time Adaptive Intelligent Control System for Quadcopter Unmanned Aerial Vehicles With Payload Uncertainties," *IEEE Transactions on Industrial Electronics*, vol. 69, no. 2, pp. 1641–1653, Feb. 2022.

[20] C. Liu, C. Dong, Z. Zhou, and Z. Wang, "Barrier Lyapunov function based reinforcement learning control for air-breathing hypersonic vehicle with variable geometry inlet," *Aerospace Science and Technology*, vol. 96, p. 105537, Jan. 2020.

[21] M. O'Connell, G. Shi, X. Shi, K. Azizzadenesheli, A. Anandkumar, Y. Yue, and S.-J. Chung, "Neural-Fly enables rapid learning for agile flight in strong winds," *Science Robotics*, vol. 7, no. 66, p. eabm6597, May 2022.

[22] Y. Z. Weimin BAO, Zhenqiang QI, "Thoughts on the development of intelligent control technology," *SCIENTIA SINICA Informationis*, vol. 50, no. 8, pp. 1267–1272, 2020.

[23] W.-M. Bao, "Present situation and development tendency of aerospace control techniques: Present situation and development tendency of aerospace control techniques," *Acta Automatica Sinica*, vol. 39, pp. 697–702, 2014.

[24] C. Zhao and L. Guo, "Control of nonlinear uncertain systems by extended pid," *IEEE Transactions on Automatic Control*, vol. 66, no. 8, pp. 3840–3847, 2021.

[25] R. Mahony, V. Kumar, and P. Corke, "Multirotor aerial vehicles: Modeling, estimation, and control of quadrotor," *IEEE Robotics & Automation Magazine*, vol. 19, no. 3, pp. 20–32, 2012.